Role of mutant SOD1 disulfide oxidation and aggregation in the pathogenesis of familial ALS

Celeste M. Karch[a], Mercedes Prudencio[a], Duane D. Winkler[b], P. John Hart[b,c], and David R. Borchelt[a,1]

[a]Department of Neuroscience, McKnight Brain Institute, University of Florida, Gainesville, FL 32610-0235; and [b]Department of Biochemistry and the X-ray Crystallography Core Laboratory, and [c]Geriatric Research, Education, and Clinical Center, Department of Veterans Affairs, South Texas Veterans Health Care System, University of Texas Health Science Center at San Antonio, 7703 Floyd Curl Drive, San Antonio, TX 78229-3900

Communicated by Joan Selverstone Valentine, University of California, Los Angeles, CA, March 17, 2009 (received for review September 22, 2008)

Transgenic mice that model familial (f)ALS, caused by mutations in superoxide dismutase (SOD)1, develop paralysis with pathology that includes the accumulation of aggregated forms of the mutant protein. Using a highly sensitive detergent extraction assay, we traced the appearance and abundance of detergent-insoluble and disulfide cross-linked aggregates of SOD1 throughout the disease course of SOD1-fALS mice (G93A, G37R, and H46R/H48Q). We demonstrate that the accumulation of disulfide cross-linked, detergent-insoluble, aggregates of mutant SOD1 occurs primarily in the later stages of the disease, concurrent with the appearance of rapidly progressing symptoms. We find no evidence for a model in which aberrant intermolecular disulfide bonding has an important role in promoting the aggregation of mutant SOD1, instead, such cross-linking appears to be a secondary event. Also, using both cell culture and mouse models, we find that mutant protein lacking the normal intramolecular disulfide bond is a major component of the insoluble SOD1 aggregates. Overall, our findings suggest a model in which soluble forms of mutant SOD1 initiate disease with larger aggregates implicated only in rapidly progressing events in the final stages of disease. Within the final stages of disease, abnormalities in the oxidation of a normal intramolecular disulfide bond in mutant SOD1 facilitate the aggregation of mutant protein.

neurodegenerative disease | protein misfolding

ALS is a late onset neurodegenerative disease that results in progressive paralysis. A subset of (f)ALS is linked to >100 missense mutations in superoxide dismutase (SOD)1 (alssod-.org) (1). The effects of fALS mutations on the normal enzyme activity, turnover, and folding of SOD1 vary considerably (2–4). Because some SOD1 mutants retain high activity (5), and because the targeted deletion of SOD1 in mice does not induce ALS-like symptoms (6), mutant SOD1 is proposed to cause disease by the acquisition of toxic properties. One proposed gain of toxic property is the propensity of SOD1 to misfold and to interact to form high-molecular-weight (HMW) structures (7, 8).

Transgenic mice that overexpress variants of mutant human SOD1, natural and experimental, share a similar phenotype of motor neuron loss, muscle wasting, and hindlimb paralysis (9). In all SOD1 transgenic mice, the appearance of symptoms is associated with an accumulation of detergent-insoluble, sedimentable, forms of mutant SOD1 in spinal cords and brainstems, properties that are diagnostic for protein aggregation (7, 8, 10). Several groups have described the appearance of HMW, detergent-insoluble SOD1 protein complexes in SOD1 transgenic mice before the onset of paralysis, with an increase in the abundance of these species as the mice develop symptoms (7, 8, 10). A substantial fraction of the detergent-insoluble mutant SOD1 that accumulates in these tissues is aberrantly cross-linked via intermolecular disulfide linkages (7, 10–14). However, the role of disulfide bonding in aggregate formation is unclear. Several studies have suggested that such cross-linking is crucial to aggregate formation (12, 15), although we recently demonstrated that, in cell culture models, aggregated forms of mutant SOD1 can be generated in the absence of disulfide cross-linking (13).

In the present study, we have examined the solubility and extent of disulfide cross-linking through the disease course in 3 different mutant SOD1 mouse models (G93A, G37R, and H46R/H48Q). Our findings demonstrate that the cross-linking and aggregation of mutant SOD1 occurs in spinal cord tissues late in disease progression well after many other pathologic features of ALS appear. The rapid progression of symptoms is paralleled by a rapid increase in the levels of aggregated mutant protein in spinal cord tissues. Immature forms of SOD1, lacking normal intramolecular disulfide bonds, contribute to aggregate formation in both cell and mouse models. These findings suggest that late in disease progression, neural cells of the spinal cord lose the ability to prevent immature mutant SOD1 from aggregating.

Results

To determine the time course of mutant SOD1 disulfide aggregation and cross-linking, we studied 3 different transgenic SOD1 mouse models (G93A, G37R, and H46R/H48Q). For each mutant mouse model, we harvested spinal cords from multiple animals at different ages (Table S1), and then extracted the tissues in nonionic detergent (0.5% Nonidet P-40). In this assay, the detergent-insoluble fraction represents aggregated SOD1 protein (8). Immunoblotting of soluble and insoluble fractions was used to detect and quantify the level of mutant SOD1 in aggregates at each age (Fig. S1). For each SOD1 variant, aggregation was quantified, and the data were graphed as a function of the total amount of the insoluble protein at endstage (Fig. 1; Table S1). Note that variation in the age at which mice reach criteria for endstage (obvious hindlimb paralysis) introduces variability in the lifespan of the mice. For this reason, the animals killed for timed harvest may be at different stages of disease, leading to variability in aggregate loads in tissues at presymptomatic ages. G93A mice, which have the shortest lifespan, showed a rapid increase in aggregate levels over the last 30 days of life (Fig. 1*A*). Similarly, increases in aggregate levels late in disease progression were seen in G37R and H46R/H48Q mice (Fig. 1 *B* and *C*). Because G37R mice accumulate less total detergent-insoluble SOD1 than the other mutants (Fig. S2 *A* and *C*), the differential between early (120 days) and endstage disease is less. At 120 days of age, the amount of insoluble G37R SOD1 in the spinal cords was not statistically different from the amount of insoluble SOD1 in the spinal cords of mice expressing WT SOD1, rising to levels well above background only late in

Author contributions: C.M.K. and D.R.B. designed research; C.M.K. and M.P. performed research; D.D.W. and P.J.H. contributed new reagents/analytic tools; C.M.K. and D.R.B. analyzed data; and C.M.K. and D.R.B. wrote the paper.

The authors declare no conflict of interest.

Freely available online through the PNAS open access option.

[1]To whom correspondence should be addressed. E-mail: borchelt@mbi.ufl.edu.

This article contains supporting information online at www.pnas.org/cgi/content/full/0902505106/DCSupplemental.

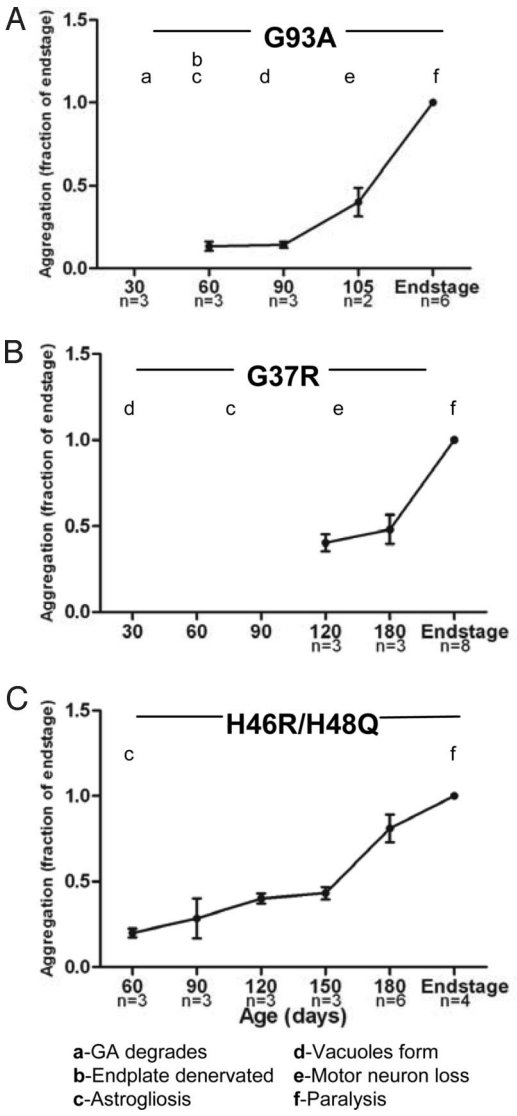

Fig. 1. Detergent-insoluble SOD1 accumulates to high levels near disease endstage. The amount of SOD1 present in the detergent-insoluble protein fraction was quantified by measuring the band intensity of SOD1 in each lane using a Fuji imaging system (FUJIFILM, LifeScience). Aggregation was quantified by calculating the ratio of band intensity in the insoluble fraction at each time point to the insoluble fraction at disease endstage (set at 1). The SEM was calculated for aggregation of each sample (Table S2) and graphed (*A*, G93A; *B*, G37R; *C*, H46RH48Q). Timelines of pathologic changes were graphed with aggregation. GA, Golgi apparatus.

disease (Fig. 1*B*). In all 3 lines of mice, the levels of mutant SOD1 in the detergent-soluble fraction remained constant as the mice aged (Fig. S1). Comparison of aggregate levels with reported pathology indicates that a number of abnormalities occur before the accumulation of aggregated SOD1 in all 3 lines of mice (Fig. 1). Less is known about the progression of disease in H46R/H48Q mice, but we have detected reactive gliosis in these mice as early as 60 days of age (Fig. S3). Thus, each SOD1 variant illustrated similar aggregation profiles throughout their lifespans; the levels of detergent-insoluble SOD1 aggregates rose during the period that symptoms rapidly progress to paralysis and well after the onset of other pathologic abnormalities.

A substantial fraction of the mutant SOD1 in HMW aggregates is cross-linked via nonnative, intermolecular, disulfide bonds (11, 12, 14). To determine whether disulfide cross-linking between misfolded SOD1 proteins occurs as a precursor to aggregate formation, spinal cords were taken at time points throughout the lifespan of G93A transgenic mice and then extracted in 1% SDS or 0.5% Nonidet P-40 in the presence of iodoacetamide (IA), a thiol modifying agent that irreversibly prevents air oxidation and disulfide bond scrambling during sample preparation. High concentrations of SDS solubilized most of the SOD1 protein (Fig. 2 *A* and *B*), which allowed for the detection of the total amount of disulfide cross-linked protein in the spinal cord at each time point (Fig. 2*B*). Disulfide cross-linked SOD1 species (dimers to multimers) were detectable at 105 days (Fig. 2*B*, lane 6), 2–3 weeks before the appearance of symptoms, but were most prominent at disease endstage in G93A mice (Fig. 2*B*, lanes 7 and 8). Extraction of these same tissue samples in 0.5% Nonidet P-40 demonstrated that cross-linked insoluble mutant SOD1 accumulated significantly late in disease (Fig. 2*C*; Fig. S4). Regardless of the method of detergent extraction used, disulfide cross-linked mutant SOD1 was virtually undetectable before 105 days of age (Fig. 2 *B* and *C*). We estimate that the disulfide cross-linked component of the detergent-insoluble protein could comprise 25 to 50% of the total aggregated mutant SOD1 (*SI Discussion* and Fig. S5). Collectively, these data demonstrate that the levels of disulfide cross-linked mutant SOD1 rise in parallel with the levels of detergent-insoluble protein, and may comprise a significant fraction of the total detergent-insoluble protein.

The coincident appearance of detergent-insoluble mutant SOD1 with disulfide cross-linked mutant protein implies a role for cross-linking in aggregation. However, extraction of the spinal cord tissue in 0.5% Nonidet P-40 with as much as 30% βME did not substantially change the amount of mutant SOD1 that partitioned into the detergent-soluble fraction (Fig. S6). Thus, although HMW species of SOD1 are extensively disulfide cross-linked, these bonds are not critical in maintaining the structure that is responsible for insolubility in Nonidet P-40.

In our study of SDS and Nonidet P-40 soluble fractions by electrophoresis in the absence of reducing agent, from mice across all ages, we observed SOD1 proteins of apparent masses of 20 and 16 kDa (Fig. 2 *B* and *D*, lanes 2–8). This banding pattern has previously been described by Jonsson et al. (11) as representing SOD1 protein in which the normal intramolecular disulfide bond between cysteines 57 and 146 is reduced (labeled, R; 20 kDa) or oxidized (labeled, O; 16 kDa) SOD1 protein. Treating the SDS and Nonidet P-40 solubilized fractions with reducing agent, before gel electrophoresis, produced a single SOD1 band that migrated at ≈20 kDa (Fig. S7 *A* and *B*). Therefore, we concluded that the spinal cords of G93A mice contained both reduced and oxidized forms of SOD1.

To confirm this finding and eliminate any potential influence of sample preparation or storage (*SI Discussion*), we harvested paralyzed animals and performed the detergent extraction and SDS/PAGE in the same day. We also included a treatment in which the gels were incubated in reducing agent before electrophoretic transfer to immunoblotting membranes. Zetterstrom et al. (16) demonstrated that the detection of oxidized forms of SOD1 by nonreducing SDS/PAGE and immunoblotting is enhanced by in-gel reduction of disulfide bonds before immunoblot transfer. In detergent-soluble fractions of tissues from both WT and endstage G93A mice, we detected both reduced and oxidized forms of monomeric SOD1. In the soluble fractions, the oxidized form of the protein represented the vast majority of detectable SOD1 protein (Fig. 3, lanes 1–4). In the insoluble fractions, no WT SOD1 was observed, and the major detectable species of mutant G93A SOD1 migrated as expected for reduced protein (Fig. 3, lanes 5–8). A second minor species of insoluble mutant SOD1 in these fractions migrated to a size similar, but not identical, to oxidized SOD1. This species was not detected when in-gel reduction before transfer was omitted (Fig. S8, lanes

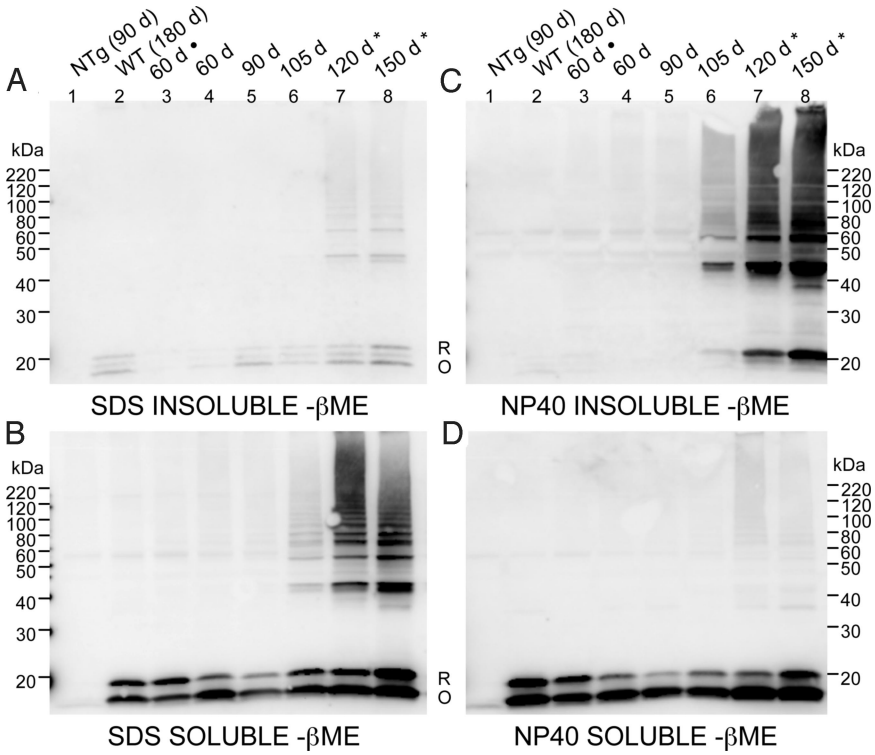

Fig. 2. The appearance of disulfide cross-linked SOD1 is coincident with the accumulation of detergent-insoluble mutant protein. G93A spinal cords were extracted in 1% SDS (*A* and *B*) or in 0.5% Nonidet P-40 (*C* and *D*) in the presence of 100 mM IA. Fractions were electrophoresed in the absence of βME. Immunoblots were probed with m/hSOD1 antiserum (representative image from 3 repetitions). NTg, nontransgenic. (*A*) Insoluble in 1% SDS (20 μg). (*B*) Soluble in 1% SDS (5 μg). (*C*) Insoluble in 0.5% Nonidet P-40. (*D*) Soluble in 0.5% Nonidet P-40. R, reduced disulfide bond (C57-C146). O, oxidized disulfide bond (C57-C146). *, disease endstage (paralysis); ·, fresh spinal cord tissue.

5–8). Whether this insoluble form of mutant SOD1 (Fig. 3, marked by #) possesses a disulfide bond between cysteines 57 and 146 is uncertain. It is possible that an intramolecular disulfide bond between other cysteine residues produced this species of mutant, insoluble SOD1. Similarly, we found significant levels of reduced mutant SOD1 in the detergent-insoluble fraction of tissues from endstage G37R and H46R/H48Q mice (Fig. S9). It is noteworthy that in these gels, the amount of HMW, disulfide cross-linked, SOD1 species detected in the detergent-insoluble fractions in these experiments was much lower, an illustration of the overall variability in the abundance of the disulfide cross-linked species that we have noted throughout these experiments (Fig. S4). Overall, we conclude that a portion of the mutant SOD1 that accumulates as detergent-insoluble is derived from protein that either never acquired, or that lost, the normal intramolecular disulfide bond.

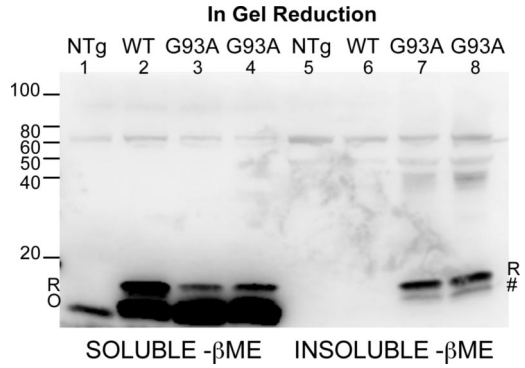

Fig. 3. SOD1 aggregates are largely composed of disulfide-reduced forms of SOD1 in fresh spinal cord tissue. Spinal cords from freshly harvested mice were extracted in nonionic detergent and IA. Gels were incubated in reducing buffer before transfer. (Lanes 1–4) Detergent-soluble (40-μg protein). (Lanes 5–8) Detergent-insoluble (40-μg protein). Immunoblots were probed with m/hSOD1 antiserum. R, reduced. O, oxidized. #, possible nonnatively oxidized bond. For additional repetitions, see Fig. S7.

To further explore the role of reduced and oxidized mutant SOD1 in aggregation, we used a cell culture model that utilizes HEK293FT cells (8, 13, 17). High-level expression in these cells induced the formation of detergent-insoluble mutant SOD1 (A4V, G37R, and G93A; Fig. 4). We included purified dimeric, metallated, WT human SOD1 as a control (Fig. 4, lanes 1 and 8 of each gel; these proteins were not subjected to detergent extraction). Reduction and denaturation of this purified protein produced a single band that migrated at ≈20 kDa (Fig. 4, lane 1), whereas denaturation and SDS/PAGE in the absence of reducing agent produced a single band that migrated at ≈16 kDa (Fig. 4, lane 8). The oxidized form of purified WT SOD1 was not detected when in-gel reduction was omitted before transfer (Fig. S10 *A* and *B*, lane 8) (16). Detergent-insoluble mutant SOD1 migrated in SDS/PAGE, after boiling in SDS, to a size close to the reduced forms of purified WT SOD1 (Fig. 4*A*). In these experiments, similar to previous studies (8), the H46R/H48Q mutant produced the least amount of detergent-insoluble protein in cell culture. In the detergent-soluble fractions of these cell extracts, we detected both reduced and oxidized forms of SOD1 in gels subjected to in-gel reduction (Fig. 4*B*, lanes 3–7). Omission of the in-gel reduction diminished detection of the oxidized form of detergent-soluble SOD1 as reported by Zetterstrom (Fig. S10*B*, lanes 3–8) (16). In analyzing the detergent-soluble fractions in the blots that included the in-gel reduction, we

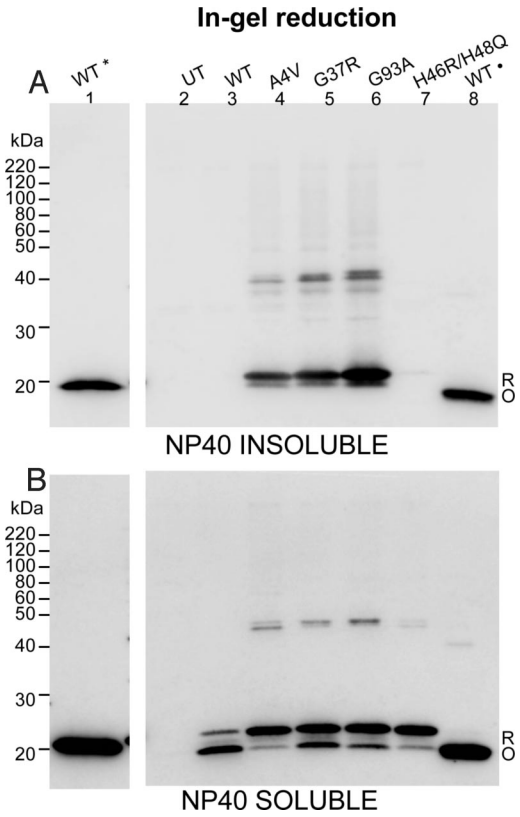

Fig. 4. Reduced hSOD1 protein is preferentially incorporated into detergent-insoluble aggregates. HEK293FT cells were transfected with vectors for WT, A4V, G37R, G93A, and H46R/H48Q hSOD1 proteins, harvested after 48 h, and extracted in buffers with 0.5% Nonidet P-40 and 100 mM IA (representative experiment from 4 repetitions). Detergent-insoluble (*A*) and soluble fractions (*B*) from cells transfected with each construct were electrophoresed in the absence of βME (lanes 2–8). Lane 1 of each panel contains purified WT SOD1 that was reduced before electrophoresis (*). This lane was separated from the remaining samples by a lane containing marker proteins and an empty space to prevent reducing agent from diffusing into other samples (these intervening lanes have been cropped out of the gel image). Lane 8 of each panel contains purified WT SOD1 that was verified to have in intact intramolecular disulfide bond (·). Purified WT SOD1 proteins were treated with 100 mM IA prior boiling in Sample buffer and electrophoresis. To enhance detection of oxidized forms of hSOD1, gels were incubated in transfer buffer containing 2% βME for 10 min before electrotransfer to nitrocellulose membranes. UT, untransfected cells; R, reduced disulfide bond (C57-C146). O, oxidized disulfide bond (C57-C146).

noted that the relative ratio of reduced to oxidized SOD1 differed between the mutant and WT SOD1 proteins. The predominant form of WT SOD1 in these transfected cells migrated to the same position as purified oxidized SOD1 (Fig. 4*B*, lanes 3 and 8). For each of the mutants, the predominant form of soluble protein migrated to the position of reduced WT SOD1 (Fig. 4*B*, lanes 1 and 4–7). For the A4V and H46R/H48Q mutants, the majority of detergent-soluble protein migrated to the same position as reduced WT protein. Together, these findings demonstrate that, in this cell culture model, mutant SOD1 is less able to acquire the normal intramolecular disulfide bond, with this reduced protein forming detergent-insoluble complexes.

Discussion

The spinal cords of paralyzed mice that express fALS-linked SOD1 mutants contain disulfide cross-linked aggregates of mutant SOD1 that are distinguished by insolubility in nonionic detergent (11, 12, 14). In the present study, we demonstrate, in 3 lines of mutant SOD1 transgenic mice (G93A, G37R, and H46R/H48Q), that SOD1 aggregates accumulate to high levels just before hindlimb paralysis, but well after the appearance of several pathologic features. Because the method we use here is relatively sensitive, we conclude that many pathologic events in the progression of disease in these mice must be mediated either by very low levels of HMW-SOD1 aggregates or by forms of mutant protein other than large aggregates.

We also investigate the role of disulfide cross-linking in mutant SOD1 aggregation, finding that the appearance of disulfide cross-linked mutant SOD1 parallels the appearance of detergent-insoluble protein. We find no evidence that disulfide cross-linked forms of SOD1 are precursors to more highly structured aggregates or that an oxidative event occurs early in the disease course to induce disulfide cross-linking between mutant proteins. Also, we demonstrate that detergent insolubility does not depend on maintenance of aberrant intermolecular disulfide bonds (Fig. S6). This finding is consistent with our previous study, which demonstrated that mutant forms of SOD1 that are incapable of forming disulfide cross-links retain the ability to aggregate (13). We conclude that disulfide cross-linking is likely a secondary event in the formation of mutant SOD1 aggregates, forming after the mutant SOD1 proteins come into close proximity as a result of assembly into HMW structures.

In both the mouse and cell models of SOD1 aggregation, we found that a fraction of the mutant SOD1 in aggregates exhibits electrophoretic properties of fully reduced SOD1 protein. This outcome is consistent with the studies of Jonsson et al. (11), which demonstrated that a significant fraction of the total SOD1 in spinal cords of transgenic mice producing D90A, G93A, and G127X variants of SOD1 lacks the normal intramolecular disulfide bond (C57-C146). More recent studies in vitro demonstrated that completely reduced forms of mutant SOD1 were most prone to produce filamentous aggregates (18), and that reduced forms of SOD1 promote aggregation of SOD1 in other oxidation states (19). Collectively, these studies argue that fully reduced species of SOD1 protein are prone to assemble into multimeric structures. Our data on the H46R/H48Q mutant, which does not bind Cu (20), is consistent with this hypothesis, because we find that most of this mutant protein, whether soluble or insoluble, exhibits an electrophoretic migration expected for fully reduced protein. Evidence suggests that copper is required to form the normal intramolecular disulfide bond (21), which could explain why the H46R/H48Q mutant fails to oxidize a cysteine 57 to 146 linkage. Importantly, the behavior of the H46R/H48Q mutant demonstrates that failure to form the normal disulfide linkage is not sufficient to induce aggregation, because most of this mutant protein remains soluble whether extracted from mouse tissues or cultured cells. Overall, these findings support a hypothesis in which mutant SOD1 that has either failed to mature properly (with respect to formation of intramolecular disulfide bonds and probably metal cofactors) or has lost these modifications is more prone to produce conformations that support aggregation (22).

In the cell model we use here, the majority of detergent soluble and insoluble mutant SOD1 showed electrophoretic mobilities consistent with reduced SOD1. Proescher et al. (23) also observed an accumulation of disulfide-reduced SOD1 when mutant SOD1 was overexpressed in HEK293 cells. In our study, it appears that the high level of expression of the mutant protein overwhelms the ability of the cells to provide the necessary factors to correctly modify most of this protein. By contrast, in spinal cords of the WT, G37R, and G93A mice, the majority of detergent-soluble SOD1 shows electrophoretic characteristics consistent with the presence of the normal intramolecular

disulfide bond. We observed no obvious increase in the relative amount of reduced, detergent-soluble, mutant SOD1 in the spinal cords of mutant mice at advanced ages, indicating that there was not a catastrophic decrease in the normal maturation of mutant protein in vivo in all cell types.

Several groups have described SOD1 aggregation in mutant SOD1 transgenic mice through various stages of disease (7, 11). In a previous study of G93A mice, detergent-insoluble protein complexes were described to increase linearly through the lifespan of the mouse, and were detected as early as 30 days (7). In this study, aggregates were defined as HMW species that were resistant to heat, SDS, and reducing agents, and they were unique to mice expressing G93A SOD1 (7). These forms of mutant SOD1 are distinct from the Nonidet P-40-insoluble protein we have studied here. It is unclear whether the HMW species of mutant SOD1 that are resistant to SDS, heat, and reducing agents represent forms of mutant protein that are covalently cross-linked to other proteins (such as ubiquitin) (8, 24), or some type of highly stable oligomeric structure. However, evidence indicates that these SDS, heat, reducing agent resistant species of mutant protein are components of Nonidet P-40-insoluble aggregates (8, 13, 24).

A previous study of insoluble SOD1 proteins in mice expressing G93A, G127X, and G85R fALS variants of SOD1 reported dramatic increases in detergent-insoluble SOD1 late in disease (11). In this study, spinal cords were extracted in low concentrations of nonionic detergent (0.1% Nonidet P-40), which resulted in the detection of detergent-insoluble species of mutant SOD1 as early as 50 days (11, 14). However, similar levels of insoluble WT SOD1 were detected in mice that overexpress human WT SOD1 at all time points (11). At disease endstage, the levels of mutant SOD1 that were Nonidet P-40-insoluble increased dramatically, including HMW forms of mutant SOD1 that were resistant to SDS, heat, and reducing agent (11). In mice expressing WT SOD1 at very advanced ages (400 to 600 days), the levels of Nonidet P-40-insoluble WT SOD1 were observed to increase with the appearance of HMW species that were SDS, heat, and reducing agent resistant (11). Thus, the methodology used in the Jonsson study (11) suggested that both mutant and WT SOD1 adopt similar conformations as a function of age. Because we use higher detergent concentrations, and possibly also much higher detergent-to-protein ratios (*SI Discussion*), we suggest that our method allows us to more selectively distinguish the misfolded forms of mutant SOD1. In an earlier study, Johnston et al. (7) reported finding SDS, heat, and reducing agent resistant HMW forms of G93A SOD1 in mouse spinal cords as early as 30 days of age. This finding implies that conformational abnormalities in mutant SOD1 occur early in disease pathogenesis. However, these abnormal forms of G93A SOD1 were of relatively low abundance at young ages, a finding we corroborate here. Despite the methodological differences between our approach and that of comparable studies, there is general agreement that the levels of mutant SOD1 aggregates (defined by any means) increase dramatically toward the terminal stages of disease.

Previous studies have established that fALS mice develop significant pathology before the appearance of hindlimb paralysis. In G93A mice, ≈40% of the motor endplates are denervated at 47 days (25), 80 days before the appearance of hindlimb paralysis and significant SOD1 aggregation. Motor unit loss (40 days; see ref. 26) and a decline in contractile force of fast twitch muscles (40 days; see ref. 27) also occur, illustrating that dramatic loss of muscle function and motor neuron innervation occurs early in the disease course. G37R mice show vacuolar changes in spinal cord (36 days; see refs. 28 and 31), motor neuron loss (133 days; see ref. 29), and reactive astrogliosis (77 days; see ref. 29) before developing hindlimb paralysis (210 days). The H46R/H48Q mice are less well characterized, but we have noted the appearance of astrogliosis in spinal cords as early as 60 days (Fig. S3). Our data indicate that, at time points when these mice have significant pathologic abnormalities, only low levels of detergent-insoluble SOD1 can be detected. A recent study demonstrated that coexpression of human copper chaperone for SOD1 (CCS) with SOD1-G93A, hastens the onset of disease and while diminishing aggregate formation and augmenting vacuolar degeneration (30). Collectively, these outcomes imply that other forms of mutant SOD1 may mediate toxic events at early stages of disease or that very low levels of aggregates are sufficient to mediate toxicity.

The late accumulation of HMW SOD1 aggregates in the disease progression in fALS mice leaves open 3 possibilities for SOD1 aggregate function in ALS pathology. First, the accumulation of SOD1 aggregates may mediate all aspects of toxicity with early pathologic events mediated by very low levels of aggregates. Second, all toxic events are mediated by soluble forms of mutant SOD1 (monomeric or oligomeric). In this scenario, aggregates form, because the toxic processes that occur in affected cell types leave them less able to properly modify nascent mutant SOD1. These immature SOD1 proteins then become the building blocks of aggregates, which are simply biomarkers for extreme cell stress. Third, soluble forms of mutant SOD1 (monomeric or oligomeric) trigger early pathologic abnormalities (gliosis, vacuolation, denervation, etc.) with the resulting stress on the cell inducing the formation of SOD1 aggregates. These aggregates then mediate additional toxic events that lead to paralytic phenotypes. Unraveling the true role of SOD1 aggregation in SOD1-linked fALS may require the identification of small molecules that selectively inhibit SOD1 aggregation, or the identification of disease-linked variants of SOD1 that do not form insoluble aggregates.

Methods

Transgenic Mice. The SOD1 transgenic mice used in this study have been previously characterized: the G93A variant [B6SJL-TgN (SOD1-G93A)1Gur; onset 4–5 mo; The Jackson Laboratory], the G37R variant [line 29 (onset 7–8 mo)] (31), the H46R/H48Q variant [line 139 (onset 6–7 mo)] (24), and the WT variant (line 76) (31). The studies here included tissues that had been in storage for extended intervals, as well as tissues harvested and used within a few days (Table S1). The length of tissue storage had no obvious effect on study outcomes (*SI Discussion*).

SOD1 Aggregation Assay by Differential Extraction. The procedures used to assess SOD1 aggregation by differential detergent extraction and centrifugation in cell culture and mouse models were similar to previous descriptions (8, 13). In variations, samples were extracted in the presence of 100 mMIA; and in some experiments, SDS was substituted for Nonidet P-40 in all extraction buffers: 1× SDS buffer (10 mM Tris pH 7.5/1 mM EDTA/100 mM NaCl/1% SDS/1× protease inhibitor mixture). Based on protein concentration, measured in both fractions by BCA method as described by the manufacturer (Pierce), 5 μg of total protein from the detergent-soluble fraction and 20 μg of total protein from the detergent-insoluble fraction were analyzed.

Immunoblotting. Standard SDS/PAGE was performed in 18% Tris-Glycine gels (Invitrogen). Samples were boiled for 5 min in Laemmli sample buffer before electrophoresis (32). In some experiments, the reducing agent (5% βME) was omitted from the sample buffer. In experiments requiring in gel reduction, before electrotransfer to nitrocellulose membranes, gels were incubated in transfer buffer in the presence of 2% βME. Immunoblots were probed with rabbit polyclonal antibodies: hSOD1 and m/hSOD1 (1:2,500). The hSOD1 antiserum recognizes human SOD1 (amino acid 24–36) (33). The m/hSOD1 antiserum recognizes mouse and human SOD1 (amino acid 124–136) (2).

ACKNOWLEDGMENTS. We thank Hilda Brown (University of Florida) for advice and assistance in generating the SOD1 expression constructs, Susan Fromholt (University of Florida) for assistance in genotyping the mice, and our colleagues for thoughtful discussions. This work was supported by National Institutes of Health Grant P01 NS049134 (to P.J.H. and D.R.B.).

1. Rosen DR, et al. (1993) Mutations in Cu/Zn superoxide dismutase gene are associated with familial amyotrophic lateral sclerosis. *Nature* 362:59–62.
2. Borchelt DR, et al. (1994) Superoxide dismutase 1 with mutations linked to familial amyotrophic lateral sclerosis possesses significant activity. *Proc Natl Acad Sci USA* 91:8292–8296.
3. Potter SZ, Valentine JS (2003) The perplexing role of copper-zinc superoxide dismutase in amyotrophic lateral sclerosis (Lou Gehrig's disease). *J Biol Inorg Chem* 8:373–380.
4. Valentine JS, Hart PJ (2003) Misfolded CuZnSOD and amyotrophic lateral sclerosis. *Proc Natl Acad Sci USA* 100:3617–3622.
5. Ratovitski T, et al. (1999) Variation in the biochemical/biophysical properties of mutant superoxide dismutase 1 enzymes and the rate of disease progression in familial amyotrophic lateral sclerosis kindreds. *Hum Mol Genet* 8:1451–1460.
6. Reaume AG, et al. (1996) Motor neurons in Cu/Zn superoxide dismutase-deficient mice develop normally but exhibit enhanced cell death after axonal injury. *Nat Genet* 13:43–47.
7. Johnston JA, Dalton MJ, Gurney ME, Kopito RR (2000) Formation of high molecular weight complexes of mutant Cu, Zn-superoxide dismutase in a mouse model for familial amyotrophic lateral sclerosis. *Proc Natl Acad Sci USA* 97:12571–12576.
8. Wang J, et al. (2003) Copper-binding-site-null SOD1 causes ALS in transgenic mice: Aggregates of non-native SOD1 delineate a common feature. *Hum Mol Genet* 12:2753–2764.
9. Turner BJ, Talbot K (2008) Transgenics, toxicity and therapeutics in rodent models of mutant SOD1-mediated familial ALS. *Prog Neurobiol* 85:94–134.
10. Wang J, Xu G, Borchelt DR (2002) High molecular weight complexes of mutant superoxide dismutase 1: Age-dependent and tissue-specific accumulation. *Neurobiol Dis* 9:139–148.
11. Jonsson PA, et al. (2006) Disulphide-reduced superoxide dismutase-1 in CNS of transgenic amyotrophic lateral sclerosis models. *Brain* 129:451–464.
12. Furukawa Y, et al. (2006) Disulfide cross-linked protein represents a significant fraction of ALS-associated Cu, Zn-superoxide dismutase aggregates in spinal cords of model mice. *Proc Natl Acad Sci USA* 103:7148–7153.
13. Karch CM, Borchelt DR (2008) A limited role for disulfide cross-linking in the aggregation of mutant SOD1 linked to familial amyotrophic lateral sclerosis. *J Biol Chem* 283:13528–13537.
14. Jonsson PA, et al. (2004) Minute quantities of misfolded mutant superoxide dismutase-1 cause amyotrophic lateral sclerosis. *Brain* 127:73–88.
15. Banci L, et al. (2007) Metal-free superoxide dismutase forms soluble oligomers under physiological conditions: A possible general mechanism for familial ALS. *Proc Natl Acad Sci USA* 104:11263–11267.
16. Zetterstrom P, et al. (2007) Soluble misfolded subfractions of mutant superoxide dismutase-1s are enriched in spinal cords throughout life in murine ALS models. *Proc Natl Acad Sci USA* 104:14157–14162.
17. Wang J, Xu G, Borchelt DR (2006) Mapping superoxide dismutase 1 domains of non-native interaction: Roles of intra- and intermolecular disulfide bonding in aggregation. *J Neurochem* 96:1277–1288.
18. Furukawa Y, et al. (2008) Complete loss of post-translational modifications triggers fibrillar aggregation of SOD1 in the familial form of amyotrophic lateral sclerosis. *J Biol Chem* 283:24167–24176.
19. Chattopadhyay M, et al. (2008) Initiation and elongation in fibrillation of ALS-linked superoxide dismutase. *Proc Natl Acad Sci USA* 105:18663–18668.
20. Wang J, et al. (2007) Disease-associated mutations at copper ligand histidine residues of superoxide dismutase 1 diminish the binding of copper and compromise dimer stability. *J Biol Chem* 282:345–352.
21. Furukawa Y, Torres AS, O'Halloran TV (2004) Oxygen-induced maturation of SOD1: A key role for disulfide formation by the copper chaperone CCS. *EMBO J* 23:2872–2881.
22. Hart PJ (2006) Pathogenic superoxide dismutase structure, folding, aggregation and turnover. *Curr Opin Chem Biol* 10:131–138.
23. Proescher JB, Son M, Elliott JL, Culotta VC (2008) Biological effects of CCS in the absence of SOD1 enzyme activation: Implications for disease in a mouse model for ALS. *Hum Mol Genet* 17:1728–1737.
24. Wang J, et al. (2002) Fibrillar inclusions and motor neuron degeneration in transgenic mice expressing superoxide dismutase 1 with a disrupted copper-binding site. *Neurobiol Dis* 10:128–138.
25. Fischer LR, et al. (2004) Amyotrophic lateral sclerosis is a distal axonopathy: Evidence in mice and man. *Exp Neurol* 185:232–240.
26. Kennel PF, Finiels F, Revah F, Mallet J (1996) Neuromuscular function impairment is not caused by motor neurone loss in FALS mice: An electromyographic study. *NeuroReport* 7:1427–1431.
27. Hegedus J, Putman CT, Gordon T (2007) Time course of preferential motor unit loss in the SOD1 G93A mouse model of amyotrophic lateral sclerosis. *Neurobiol Dis* 28:154–164.
28. Borchelt DR, et al. (1998) Axonal transport of mutant superoxide dismutase 1 and focal axonal abnormalities in the proximal axons of transgenic mice. *Neurobiol Dis* 5:27–35.
29. Watanabe M, et al. (2001) Histological evidence of protein aggregation in mutant SOD1 transgenic mice and in amyotrophic lateral sclerosis neural tissues. *Neurobiol Dis* 8:933–941.
30. Son M, et al. (2007) Overexpression of CCS in G93A-SOD1 mice leads to accelerated neurological deficits with severe mitochondrial pathology. *Proc Natl Acad Sci USA* 104:6072–6077.
31. Wong PC, et al. (1995) An adverse property of a familial ALS-linked SOD1 mutation causes motor neuron disease characterized by vacuolar degeneration of mitochondria. *Neuron* 14:1105–1116.
32. Laemmli UK (1970) Cleavage of structural proteins during the assembly of the head of bacteriophage T4. *Nature* 227:680–685.
33. Bruijn LI, et al. (1997) ALS-linked SOD1 mutant G85R mediates damage to astrocytes and promotes rapidly progressive disease with SOD1-containing inclusions. *Neuron* 18:327–338.